

connected with the excitation of the echo signals by the fronts of the applied pulses. Thus, when series of two pulses of durations 10^{-6} sec and 4×10^{-8} sec and in the opposite sequence were applied, we observed the distorted signals shown in Fig. 4. The intensity of the former case is higher, because the power of the short pulse was larger, and the intensity of the echo signal is proportional according to (1) to $E_1 E_2^2$.

The considered spectral approach enables us to explain the singularities of formation of echo signals by two microwave pulses with linear frequency modulation $\omega(t) = \omega_0 + \beta t$, $\omega_0 + \beta' t$, where β and β' are the modulation rates of the first and second pulses. The spectral density of the linearly modulated microwave pulse can be represented in the form¹⁴

$$G_1(\omega) = \frac{E_1 T_c}{2^{3/2} m} \exp \left[-\frac{i(\omega - \omega_0)^2}{2\beta} \right] \{C(u_1) + C(u_2) + i[S(u_1) + S(u_2)]\},$$

where T_c is the pulse duration, $m = \beta T_c^2 / 2\pi$, $C(u)$ and $S(u)$ are Fresnel integrals. At large values of m and $\omega = \omega_0$ we get $C(u_1) \approx S(u_2) \approx 0.5$. Substituting these values for the first and second pulses in (2), we find that the spectral density of the echo signal is proportional to

$$\exp \left[-\frac{i(\omega - \omega_0)^2}{2} \left(\frac{1}{\beta} - \frac{2}{\beta'} \right) \right].$$

The spectrum is nearly rectangular, and at $\beta' = 2\beta$ the phase is constant, corresponding for the time picture to a compression of the echo signal in the absence of fre-

quency modulation.

- ¹A. L. Bloom, *Phys. Rev.* **98**, 1105 (1955).
- ²P. F. Liao and S. R. Hartmann, *Phys. Lett. A* **44**, 361 (1973).
- ³Yu. M. Bun'kov, B. S. Dumesh, and M. I. Kurkin, *Pis'ma Zh. Eksp. Teor. Fiz.* **19**, 216 (1974) [*JETP Lett.* **19**, 132 (1974)].
- ⁴R. W. Gould, *Phys. Lett.* **19**, 477 (1965).
- ⁵B. D. Laikhtman, *Fiz. Tverd. Tela (Leningrad)* **18**, 612 (1976) [*Sov. Phys. Solid State* **18**, 357 (1976)].
- ⁶V. M. Berezov, V. I. Bashkov, V. D. Korepanov, and V. S. Romanov, *Zh. Eksp. Teor. Fiz.* **73**, 257 (1977) [*Sov. Phys. JETP* **46**, 133 (1977)].
- ⁷S. A. Zel'dovich and A. R. Kessel', *Fiz. Tverd. Tela (Leningrad)* **19**, 1464 (1977) [*Sov. Phys. Solid State* **19**, 853 (1977)].
- ⁸K. Fossheim, K. Kajimura, T. G. Kazyaka, R. L. Melcher, and N. S. Shiren, *Phys. Rev. B* **17**, 964 (1978).
- ⁹P. A. Fedders and E. Y. C. Lu, *Appl. Phys. Lett.* **23**, 502 (1970).
- ¹⁰U. Kh. Kopvillem, B. P. Smolyakov, and R. Z. Sharipov, *Pis'ma Zh. Eksp. Teor. Fiz.* **13**, 558 (1971). [*JETP Lett.* **13**, 398 (1971)].
- ¹¹L. Billmann, Ch. Frenois, J. Joffrin, A. Livelut, and S. Ziolkiewich, *J. Phys.* **34**, 453 (1973).
- ¹²B. P. Smolyakov, E. I. Shtyrkov, and B. Z. Malkin, *Zh. Eksp. Teor. Fiz.* **74**, 1053 (1978) [*Sov. Phys. JETP* **47**, 553 (1978)].
- ¹³W. B. Mims, *Phys. Rev.* **141**, 499 (1966).
- ¹⁴I. S. Gonorovskii, *Radiotekhnicheskie tsepi i signaly (Radio Circuits and Signals)*, Sovetskoe Radio, 1977.

Translated by J. G. Adashko

Field-ion-microscopy study of collective field-emission evaporation of tungsten atoms

I. M. Mikhaïlovskii, Zh. I. Dranova, V. A. Ksenofontov, and V. B. Kul'ko

Khar'kov Physicotechnical Institute, Ukrainian Academy of Sciences

(Submitted 10 August 1978)

Zh. Eksp. Teor. Fiz. **76**, 1309-1315 (April 1979)

Field ion microscopy is used to investigate the kinetics of evaporation of tungsten in an electric field at temperatures 21-180 K in the evaporation-rate interval 10^{-4} - 10^{-7} Å/sec. Below 110 K, the average rate of desorption of atoms from the (110) face increases by more than two orders of magnitude when the dimensions of the atomic complexes decreases. It is observed that at 110 K the collective desorption changes into separate-atom desorption. The collective desorption is attributed to a shift of the effective electron surface because of the increase of the electron density with decreasing dimensions of the atomic complexes.

PACS numbers: 79.70. + q, 07.80. + x, 82.65.My

Field-ion-microscopy study of the kinetics of low-temperature evaporation of metals in electric fields 10^8 - 10^9 V/cm (Ref. 1) yields data on the electron structure of metals,² on the dynamics of surface atoms,³ and on the effect of various physical processes in strong electric fields on the formation of the ion field-emission image.^{1,4} It is known that in the course of field evaporation of atoms from close-packed faces the rate of evaporation increases sharply after the atomic complex reaches a certain critical size.^{5,6} To determine the mechanism of this phenomenon, we have investigated in

the present paper the singularities of the field evaporation kinetics of tungsten from the {110} face, in a wide evaporation-rate interval (10^{-4} - 10^7 Å/sec), using ion field emission microscopy.

EXPERIMENTAL PROCEDURE AND RESULTS

The samples were subjected to an electric field produced by a 5-30 kV dc source and a series-connected generator of pulses of duration 2×10^{-7} - 2×10^{-5} sec and amplitude 0-10 kV. When the acceleration is by a dc

voltage in the interval of velocities (k_e) from 10^{-4} to $1 \text{ \AA}/\text{sec}$, the measurements were made visually, by counting the atomic $\{110\}$ layers evaporated after a definite time: at k_e from 10^{-1} to $10 \text{ \AA}/\text{sec}$ we used motion-picture photography with preliminary amplification of the brightness of the image by a factor 10^4 ; oscillograms of the evaporation of the $\{110\}$ face were taken in the case $k_e > 10 \text{ \AA}/\text{sec}$. At $k_e > 10^2 \text{ \AA}/\text{sec}$ the measurements were made under pulsed conductions by counting the number of pulses of given duration needed to evaporate one atomic layer. The temperature of the tip was varied by passing current through the sample holder. The temperature in the interval $21\text{--}180 \text{ K}$ was determined by measuring the threshold voltage of the evaporating field of the tungsten.⁷

The ion charge was determined with an ion-emission microanalyzer⁸; the samples were evaporated by two high-voltage nanosecond pulses, the first of which produces desorption and the second does the analyzing. The $10^{-4}\text{--}10^{-5}$ delay between the pulses ensured that the mass analysis was performed on a practically pure surface. The exposure of the samples in the residual gas at a pressure $10^{-7}\text{--}10^{-6}$ Torr was $10^{-6}\text{--}10^{-5}$ Langmuir units, corresponding the performance of mass spectrometric measurements in ultrahigh vacuum.

At temperatures below 110 K , in samples having a curvature radius R larger than 200 \AA , in the entire investigated evaporation-rate interval, a jumplike increase of the evaporation rate was observed when the atomic complex reached a radius $10\text{--}15 \text{ \AA}$. Figure 1 shows the dependence of the ratio of the tangential evaporation rate dr/dt (r is the average radius of the central $\{110\}$ atomic ring) to the normal rate k_e of evaporation of the material along the sample axis on the quantity r/r_{max} , where r_{max} is the average radius of the atomic ring immediately after the evaporation of the preceding $\{110\}$ atomic layer. The data presented were obtained for samples with curvature radii $R = 90$ and 300 \AA in the vicinity of the investigated face, under constant conditions ($T = 78 \text{ K}$). When the dimension of the complex is decreased to $(0.45\text{--}0.50)r_{\text{max}}$ the evaporation rate of the samples with $R = 300 \text{ \AA}$ radius increased by 500 times and more. A complex of atoms with $r < 0.45r_{\text{max}}$ takes place in a time corresponding to the average evaporation time of one atom, and can be regarded as a collective process. No collective evaporation was observed in samples with a curvature radius

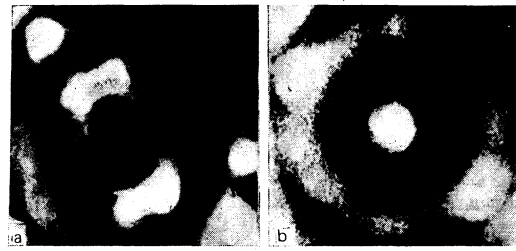


FIG. 2. Atomic complexes of critical size at the center of the $\{110\}$ face of tungsten at evaporation temperatures 78 K (a) and 120 K (b); $R = 270 \text{ \AA}$, $k_e = 10^{-2} \text{ \AA}/\text{sec}$.

less than 100 \AA at 78 K , in the entire investigated interval of evaporation rates $10^{-4}\text{--}10^7 \text{ \AA}/\text{sec}$. Decreasing the dimension of the evaporated atomic ring is accompanied by an increase of the tangential velocity, which, however, is not jumplike (Fig. 1). The atoms are evaporated separately.

Evaporation under pulsed conditions, corresponding to a normal evaporation rate $10^2\text{--}10^7 \text{ \AA}/\text{sec}$, is similar in character. At a total number of evaporating pulses exceeding 10^3 in samples with $R > 200 \text{ \AA}$, in no case was a complex observed with a dimension smaller than $0.4r_{\text{max}}$, thus indicating a collective character of the desorption of the groups of atoms of submicroscopic dimensions.

At temperatures above 110 K , the collective evaporation changes into evaporation of separated atoms: the last to be desorbed from the $\{110\}$ face are one or two atoms of tungsten (Fig. 2). The temperature dependence of the critical dimension r_{cr} corresponding to the smallest registered average radius of the desorbed complex of atoms, for a tip of 270 \AA radius, is shown in Fig. 3. The section in which r_{cr} decreases sharply with increasing temperature near 110 K corresponds apparently to a change in the desorption mechanism, accompanied by a change of the stability in the electric field of individual atoms on the $\{110\}$ face.

For a quantitative estimate of the relative stability of the atoms, the samples were evaporated at 200 K , i. e. under conditions of separate-atom evaporation, until a configuration is produced with one tungsten atom at the center of the investigated face. The samples were then cooled to 78 K , the field intensity was increased at a rate $10^{-2} \text{ V} \cdot \text{ \AA}^{-1} \cdot \text{ sec}^{-1}$, and the field intensities E_d of atom desorption from the center of the face and E_e of

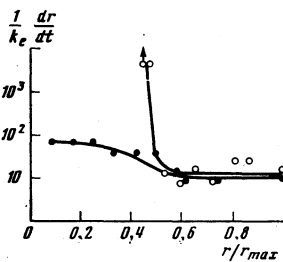


FIG. 1. Dependence of the relative field-evaporation rate of an atomic complex on its dimensions for a point radius $R = 300 \text{ \AA}$ (○) and 90 \AA (●) ($T = 78 \text{ K}$).

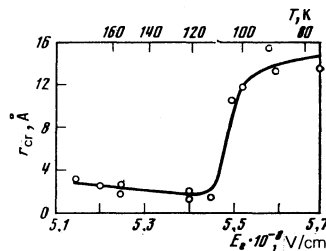


FIG. 3. Critical dimension of atomic complex vs. the temperature and the electric-field intensity corresponding to tungsten evaporation $10^{-2} \text{ \AA}/\text{sec}$ ($R = 270 \text{ \AA}$).

evaporation of the atoms from the steps on the {110} face were fixed. The values of E_0 were varied by varying the sample temperature at a constant evaporation rate. The measurements have shown that at a field intensity above 5.5 V/\AA , corresponding to a transition from separate-atom evaporation to collective evaporation, the quantity $E_d - E_0$, which determined the relative stability of the adsorbed atoms in the electric field, decrease on the average by $9 \times 10^6 \text{ V/cm}$. A comparison was made of the charges of the ions produced at 78 K at a distance $(1-2)r_{\text{max}}$ and $(0-0.4)r_{\text{max}}$ from the (110) pole. In the latter case a group of atoms with dimension less than critical was directed to the probing opening of the microanalyzer (the desorption was correspondingly collective in character). The dominant role in the spectrum of the collectively desorbed ions are triply and quadruply charged ions; the ratio of the total number of observed triply charged ions to the number of quadruply charged ones is 1.5. On the surface sections from which the atoms were separately evaporated, this ratio is 5.7.

DISCUSSION OF RESULTS

The peculiarities of atom desorption from close-packed planes are usually attributed to abrupt changes in the number of atoms on the kinks of the atomic steps as the atomic layer is being evaporated by the field.^{5,6} The transition observed in the present study, from collective evaporation from separate-atom evaporation with changing temperature, indicates that the geometric treatment discussed above is not universal. To clarify the nature of the collective evaporation it is necessary apparently to take into account the connection between the electronic structure of the surface, on the one hand, and the singularities of its microtopography, on the other. Since field evaporation is from atomic steps, the local bending of the effective electron surface can exert a substantial influence on the evaporation kinetics.

The expression that connects the kinetic energy G of an inhomogeneous electron gas in the ground state with the local electron density n , without allowance for correlation effects, is

$$G(n) = \int \left\{ \frac{3\hbar^2}{10m} (3\pi^2)^{2/3} n^{5/3} + \frac{\hbar^2 |\nabla n|^2}{72mn} \right\} dr, \quad (1)$$

where

$$n = {}^{1/2} n_0 [1 - (1 - \exp[-\lambda(|x| - \gamma y)] \text{sgn } x)], \quad (1a)$$

m is the electron mass, n_0 is the electron density in the interior of the metal, and λ and γ are parameters that determine the change of the electron density along the normal to the surface of the x axis and of the y axis parallel to it.

The first term in the integrand of (1) is the energy per unit volume of the homogeneous electron gas, the second describes the increase of the kinetic energy connected with the presence of the gradient of the electron density. For a numerical estimate of the increase of the kinetic energy $g(n)$, due to the inhomogeneity of the electron gas, referred to the unit cell of the surface lattice, we obtain from (1) and (1a), by integrating with respect to x in the interval from $-\infty$ to $+\infty$ for the cen-

ter of the atomic complex ($y = 0$):

$$g(n) = \frac{\hbar^2 n \lambda \ln 2}{72m} (\gamma^2 + 1) \Omega, \quad (2)$$

where Ω is the area per surface atom.

At the high electron densities typical of transition metals, the depth λ^{-1} of the screening of the electric field can be assumed to be¹¹

$$\lambda^{-1} = \lambda_0^{-1} + \pi/4k_F. \quad (3)$$

Here γ_0^{-1} is the depth of the Thomas-Fermi screening, k_F is the Fermi wave vector.

With decreasing dimensions of the evaporated atom group ($r \rightarrow 0$), the local curvature of the electron surface increases and the values of γ and $g(n)$ increase accordingly. It follows from (2) and (3) that the maximum value of $g(n)$ as $\gamma \rightarrow 1$, assuming that the valence of tungsten is six,¹² amounts to 0.39 eV. The increase of the kinetic energy of the electron gas with decreasing size of the complex is accompanied by a smoothing of the effective electron surface⁹ and consequently a shift of the surface towards the ion lattice. For a quantitative estimate of the shift with increasing size of the complex of evaporated atoms, we consider the potential-energy diagram of a v -fold ionized atom A^{v+} in the surface layer of a metal Me^{v+} as a function of the distance x from the effective electronic surface (Fig. 4).

As shown by Lang and Kohn,¹³ the effective electron surface of the metal is located at a distance $x_0 = d/2 + \xi(n)$ from the crystallographic plane that passes through the surface sites of the lattice [d is the distance between planes and $\xi(n)$ is a correction that takes into account the spreading of the electron gas in the near-surface region]. In the absence of an electric field, the dependence of the potential energy $U_i(v, x)$ on x is close to parabolic; the depth of the potential well at $x = x_0$ corresponds to the heat of sublimation Λ . In a strong electric field, the potential-energy curve of the $\text{Me}^{v+} + A^{v+}$ system is deformed, the equilibrium point shifts towards the surface [the point x'_0 on the $U_i(v, E, x)$ curve, Fig. 4] and two evaporation activation barriers are formed. One of them of height Q_v is located inside the metal ($x_c < 0$), and the second is the

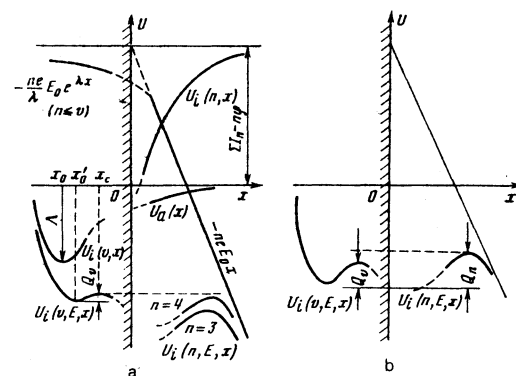


FIG. 4. Diagram of the potential energy of the $\text{Me} + A$ system. Upon evaporation in the electric field, the atom overcomes in succession the activation barriers Q_v and Q_n : a— $Q_v > Q_n$, b— $Q_v < Q_n$.

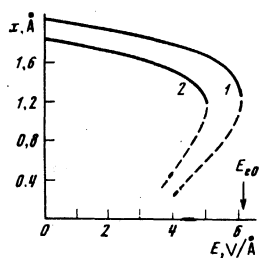


FIG. 5. Dependence of the coordinates of the equilibrium points x_0' (solid curves) and of the maxima of the evaporation activation barriers x_c (dashed curves) on the field intensity E_0 . Curves 1 and 2 correspond to $\xi = 0.93$ and 0.73 Å, respectively. E_{e0} is the intensity of the activationless evaporation field.

Schottky barrier Q_n and is located outside the metal.

In strong electric fields, the potential energy curves of the ion and of the atom, $U_i(n, E, x)$ and $U_a(x)$, respectively, do not intersect at $x > 0$, and the ground state at any distance from the effective electron surface is ionic. At distances from the surface exceeding the critical charge-exchange distance, at which electron exchange between the evaporated particle and the metal ceases, the ionic and atomic potential curves are separated,¹⁴ the ion energy $U_i(n, E, x)$ can be written, with account taken of the image forces, in the form

$$U_i(n, E, x) = \Lambda + \sum_n I_n - n\varphi - n^2 e^2 / 4x - neE_0 x, \quad (4)$$

where I_n is the n -fold ionization potential, φ is the work function, and E_0 is the field intensity on the surface of the metal. According to (4), for tungsten ions with charges 3 and 4, the Schottky barrier is higher in the investigated interval of electric fields, (3.5–6) $\times 10^8$ V/cm, than for ions with $n=6$. Therefore to explain the experimentally observed yield of triply and quadruply charged ions we must take into consideration the recombination of the sixfold charge ions at x smaller than the critical charge-exchange distance.

To analyze the dependence of the shift of the effective electron surface on the dimension of the evaporated complex we calculated the coordinates of the equilibrium points x_0' of the surface atoms and of the maxima of the evaporation activation barriers x_c as functions of the field intensity for various values of the correction, with the aid of a computer, from the equation for the potential energy of the $Me^{v+} + A^{v+}$ system, when the atom is displaced from the equilibrium position x_0 in the electric field (at $x < 0$) by an amount

$$\Delta U = \frac{1}{2} \alpha (x - x_0)^2 - ve \int_{-\infty}^x E(x) dx, \quad (5)$$

where α is the strength constant. Figure 5 shows plots of the coordinates x_0' and x_c against the field intensity E_0 . In Eq. (5) it was assumed that $E(x) = E_0 e^{\lambda x}$ (Ref. 9) and $\alpha = a \sum_{ikh}^0 b_{ikh} c_{ikh}$, where b_{ikh} are numerical coefficients that connect the force constants with the elastic moduli c_{ikh} ,¹⁵ and a is the lattice parameter. For bcc crystals we have $b_{11} = 1/2$, $b_{12} = 1/8$, and $b_{44} = 13/8$. Curve 1 was calculated for $\xi = 0.93$ Å corresponding to $r \rightarrow \infty$ (Ref. 12), and curve 2 for $\xi = 0.73$ Å. It follows from

Fig. 5 that at a certain limiting value $E_0 = E_{e0}$ corresponding to activationless evaporation by the field we have $x_c = x_0'$, and the atom equilibrium point is displaced by an amount equal to the depth λ^{-1} of penetration of the electric field into the metal. Assuming for tungsten $c_{11} = 5.33 \times 10^{12}$ dyn/cm², $c_{12} = 2.05 \times 10^{12}$ dyn/cm², and $c_{44} = 1.63 \times 10^{12}$ dyn/cm²,¹⁶ we obtain 6.20 V/Å, which is in satisfactory agreement with the experimental value $E_{e0} = 6.08$ V/Å.¹⁷

The field intensity E_{e0} decreases with the decrease of ξ which accompanies the smoothing of the electron surface. The experimentally observed, by a factor 5×10^2 , of the evaporation rate when r is decreased to $r_{cr} = 14$ Å and on going to the collective evaporation in a field $E_0 = 5.7$ V/Å at 78 K corresponds to a decrease of the activation energy Q_v by 4.2×10^{-2} eV. This decrease of Q_v can be due to an additional displacement of the effective electron surface by an amount $\Delta \xi = 6.5 \times 10^{-3}$ Å. The quantity $\Delta \xi$ is about one-tenth the theoretical shift of the effective electron surface near the projecting atoms.⁹ The difference between the displacements is apparently due to the fact that the electron gradient density is lower over the desorbed complex with dimension on the order of several lattice parameters than it is over monatomic projections.

The change in the desorption mechanism at $E_0 = 5.5$ V/Å can be attributed to a transition to the Schottky evaporation mechanism; in this case the height Q_n of the activation barrier does not depend on the position of the effective electron surface. The point of transition from the collective evaporation to the separate-atom evaporation corresponds in this case the equality $Q_v = Q_n$.

In conclusion, the authors are grateful to V.I. Gerasimenko for useful discussions of the results.

- ¹E. Muller and T. T. Tzong, *Field Ion Microscopy*, Am. Elsevier, 1969.
- ²T. T. Tzong and E. W. Müller, *Phys. Rev.* **181**, 530 (1969).
- ³I. M. Mikhailovskii and Zh. I. Dranova, *Pis'ma Zh. Eksp. Teor. Fiz.* **22**, 271 (1975) [*JETP Lett.* **22**, 125 (1975)].
- ⁴A. L. Suvorov, T. L. Razinkova, G. M. Kukavadze, A. R. Bobkov, V. Ya. Kuznetsov, and V. A. Kuznetsov, *Zh. Eksp. Teor. Fiz.* **68**, 1460 (1975) [*Sov. Phys. JETP* **41**, 729 (1975)].
- ⁵D. Brandon, in *Field Ion Microscopy*, J. H. Hren and S. Ranganathan, eds. Plenum, 1968.
- ⁶H. N. Southworth and B. Ralph, *J. Microscopy* **90**, 167 (1969).
- ⁷T. Kuroda, H. Yagi, and Sh. Nakamura, *Mem. Inst. Sci. and Ind. Res. Osaka Univ.* **26**, 101 (1969).
- ⁸R. I. Garber, E. P. Eres'ko, V. B. Kul'ko, V. A. Ksenofontov, and I. M. Mikhailovskii, *Proc. of First All-Union Conf. on Field Ion Microscopy*, Physicotechnical Inst., Ukr. Acad. Sci., Khar'kov, 1976, p. 19.
- ⁹R. Smoluchowski, *Phys. Rev.* **60**, 661 (1941); N. D. Land, *Solid State Phys.* **28**, 225 (1973).
- ¹⁰A. S. Kompaneets and E. S. Pavlovskii, *Zh. Eksp. Teor.*

Fiz. 31, 427 (1956) [Sov. Phys. JETP 4, 326 (1957)].

¹¹D. M. Newns, Phys. Rev. B 1, 3304 (1970).

¹²J. R. Smith, Phys. Rev. Lett. 25, 1023 (1970).

¹³N. D. Lang and W. Kohn, Phys. Rev. B 7, 3541 (1973).

¹⁴E. Ya. Zandberg and N. I. Ionov, Poverkhnostnaya ionizatsiya (Surface Ionization), Nauka, 1969.

¹⁵L. Dobrzyuski and P. Masri, J. Phys. Chem. Solid 33,

1603 (1972).

¹⁶F. H. Featherston and J. R. Neighbours, Phys. Rev. 130, 1324 (1963).

¹⁷T. T. Tsong and E. W. Müller, Phys. Status Solidi A 1, 513 (1970).

Translated by J. G. Adashko

Investigation of the applicability of the vortex model for bridge junctions of superconductors with the A-15 lattice

A. I. Golovashkin, A. N. Lykov, and S. L. Prishchepa

P. N. Lebedev Physics Institute, USSR Academy of Sciences

(Submitted 28 August 1978)

Zh. Eksp. Teor. Fiz. 76, 1316-1324 (April 1979)

The properties of V_3Si bridge junctions of variable thickness prepared by the double-scribing method are studied. The current-voltage characteristics (CVC) and the temperature dependence of the critical current are measured for such junctions, and the nature of the interaction of the vortex structure with a variable electromagnetic field is investigated. Characteristic current steps are observed on the CVC, and it is shown that the model based on the movement of a chain of Abrikosov vortices through the junction agrees well with the experimental data. Some parameters of the motion of the vortices are estimated on the basis of this model.

PACS numbers: 74.50. + r, 85.25. + k, 74.90. + n

INTRODUCTION

The present paper is devoted to the study of the properties of bridges made of high-temperature superconductors with the A-15 structure. The interest in these materials is due to their high critical parameters, which opens up areas of application inaccessible to ordinary superconductors. Furthermore, superconductors with the A-15 lattice possess a number of other anomalous properties,¹⁻³ and this makes them interesting objects of physical investigation. One of such properties is the smallness of the coherence length ξ_0 (~ 30 Å), which is connected with the smallness of the conduction-electron concentration. This should lead to a number of peculiarities in the manifestation of the Josephson effect in such systems.

In our previous investigations⁴⁻⁷ we studied in detail the properties of Nb_3Sn bridge junctions. It was shown that these junctions are well described by the vortex model.⁷⁻⁹ The purpose of the present investigation was to verify the generality of the vortex model for these superconductors. The investigation was carried out on bridges made of the V_3Si alloy.

The choice of V_3Si as the object of investigation is due to a number of reasons. First, this superconductor belongs to a group of vanadium high-temperature superconducting compounds whose physical characteristics differ somewhat from the characteristics of the niobium compounds. In V_3Si we have the highest value of the critical temperature T_c among the vanadium alloys. Second, as far as we know, no attempts have thus far been made to produce bridge junctions from the vanadium compounds and investigate their properties. Third, the relative closeness of the melting (and vaporization) points

of vanadium and silicon allows us to use, in preparing the alloy films, the method of vaporization from one source, which ensures higher sample homogeneity in comparison with the method of vaporization of the components from different sources.

In the present paper we propose a method for fabricating V_3Si bridges, study the temperature dependence of their critical current, the shape of the current-voltage characteristics (CVC), and the nature of the interaction of such bridge junctions with electromagnetic radiation, and determine the parameters of the vortex motion in the bridges.

EXPERIMENT

V_3Si films were prepared by the method proposed in Ref. 10. In this case the evaporation of the drop prepared by preliminary fusion of vanadium and silicon was carried out by an electron beam in a 1×10^{-5} Torr vacuum. The alloy films were deposited on heated ruby, sapphire, and quartz substrates. The optimal temperature of the substrates was 1100 °C. The rate of deposition was 100 Å/sec and the thicknesses of the prepared films were 0.2 – 0.8 μ . For the investigation we used films with sufficiently high T_c values. In the best of them T_c attained a value of 17 K (at the beginning of the transition) for a transition width of 1 K. The V_3Si microbridges were prepared by the double-scribing method.^{7,11} Bridges of width from 1 to 30 μ and length 1 – 2 μ were fabricated by this method.

The apparatus for, and the scheme of, the measurement of the temperature dependence of the critical current I_c and the CVC of the bridges are described in detail in Ref. 6. The experimental setup for the investi-